9
Basic elastostatics

Flagpoles, bridges, houses and towers are built from elastic materials, and are designed to stay in one place with at most small excursions away from equilibrium due to wind and water currents. Ships, airplanes and space shuttles are designed to move around, and their structural integrity depends crucially on the elastic properties of the materials from which they are made. Almost all human constructions and natural structures depend on elasticity for stability and ability to withstand external stresses [Vogel 1988, Vogel 1998].

It can come as no surprise that the theory of static elastic deformation, *elastostatics*, is a huge engineering subject. Engineers must know the internal stresses in their constructions in order to predict risk of failure and set safety limits, and that is only possible if the elastic properties of the building materials are known, and if they are able to solve the equations of elastostatics, or at least get decent approximations to them. Today computers aid engineers in getting precise numeric solutions to these equations and allow them to build critical structures, such as submarines, supertankers, airplanes and space vehicles, in which over-dimensioning of safety limits is deleterious to fuel consumption as well as to construction costs.

In this fairly long chapter we shall recapitulate the equations of elastostatics for bodies made from isotropic materials and apply them to the classic highly symmetric body geometries for which analytic solutions can be obtained. With the present availability of numeric simulation tools, there is no reason to spend a lot of time on more complex examples. In chapter 10 we shall apply the results to one-dimensional bodies (rods), and in chapter 11 we shall outline the principles for obtaining numeric solutions. Many specialized textbooks cover elastostatics to greater depth than here, for example [Bower 2010], [da Silva 2006], [Landau and Lifshitz 1986], [Sedov 1975].

9.1 Equations of elastostatics

Basic elastostatics concerns deformations in bodies of highly symmetric non-exceptional shapes, subjected to simple combinations of external forces. The bodies are assumed to be made from an isotropic and homogeneous linear elastic material, but even with all these assumptions it still takes some work to find the analytic solutions when it can be done at all. One of the simplest cases, the gravitational settling of a circularly cylindrical body standing on a hard horizontal floor, cannot be solved analytically, although a decent analytic approximation can be found (see section 9.2).

The fundamental equations of elastostatics are obtained from a combination of the results of the three preceding chapters,

$$f_i + \sum_j \nabla_j \sigma_{ij} = 0, \qquad \text{mechanical equilibrium (6.22)} . \tag{9.1a}$$

$$\sigma_{ij} = 2\mu\, u_{ij} + \lambda \delta_{ij} \sum_k u_{kk}, \qquad \text{Hooke's law (8.8)} \tag{9.1b}$$

$$u_{ij} = \tfrac{1}{2}\left(\nabla_i u_j + \nabla_j u_i\right), \qquad \text{Cauchy's strain tensor (7.20)} \tag{9.1c}$$

We shall only use these equations for time-independent external gravity where the body force, if present, is given by $\boldsymbol{f} = \rho \boldsymbol{g}$. The body force could also be of electromagnetic origin, for example caused by an inhomogeneous electric field acting on a polarizable dielectric.

Inserting the two last equations into the first we get in index notation,

$$\sum_j \nabla_j \sigma_{ij} = 2\mu \sum_j \nabla_j u_{ij} + \lambda \nabla_i \sum_j u_{jj} = \mu \sum_j \nabla_j^2 u_i + (\lambda + \mu)\, \nabla_i \sum_j \nabla_j u_j .$$

Rewriting this in vector notation, the equilibrium equation finally takes the form

$$\boxed{\boldsymbol{f} + \mu \nabla^2 \boldsymbol{u} + (\lambda + \mu)\, \boldsymbol{\nabla} \boldsymbol{\nabla} \cdot \boldsymbol{u} = \boldsymbol{0}.} \tag{9.2}$$

which is called *Navier's equation of equilibrium* or the *Navier–Cauchy equilibrium equation*. For the analytic calculations in this chapter it actually turns out to be more enlightening to use the three basic equations (9.1) rather than this equation.

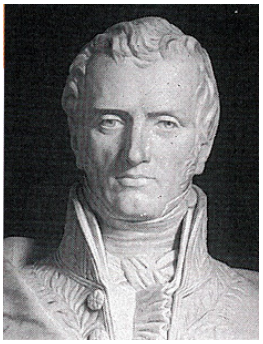

Claude Louis Marie Henri Navier (1785–1836). French engineer, worked on applied mechanics, elasticity, fluid mechanics and suspension bridges. Formulated the first version of the elastic equilibrium equation in 1821, a year before Cauchy gave it its final form.

The displacement gradients are always assumed to be tiny, allowing us to ignore all non-linear terms in the above equations, as well as to view the displacement field as a function of the original coordinates of the undeformed material rather than the actual coordinates. Effectively we use the Lagrangian representation with the spatial variable denoted $\boldsymbol{x}$ rather than $\boldsymbol{X}$. Furthermore, the linearity of the equilibrium equations allows us to *superpose* solutions. Thus, for example, if you both compress and stretch a body uniformly, the displacement field for the combined operation will simply be the sum of the respective displacement fields.

The boundary conditions are often implicit in the mere posing of an elastostatics problem. Typically, a part of the body surface is "glued" to a hard surface where the displacement has to vanish, and where the environment automatically provides the external reaction forces necessary to balance the surface stresses. On the remaining part of the body surface explicit external forces implement the "user control" of the deformation. In regions where the external forces vanish, the body surface is said to be *free*. For the body to remain at rest the total external force and the total external moment of force must always vanish.

Estimates

Confronted with partial differential equations, it is always useful to get a rough idea of the size of a particular solution. It should be emphasized that such estimates just aim to find the right orders of magnitude of the fields, and that there may be special circumstances in a particular problem which invalidate them. If that is the case, or if precision is needed, there is no way around analytic or numeric calculation.

Imagine, for example, that a body made from elastic material is subjected to surface stresses of a typical magnitude P and that the deformation of the body due to gravity can be ignored. A rough guess on order of magnitude of the stresses in the body is then also $|\sigma_{ij}| \sim P$. The elastic moduli λ, μ, E and K are all of the same magnitude, so that the deformation is of the order of $|u_{ij}| \sim P/E$, here disregarding Poisson's ratio which is anyway of order unity. Since the deformation is calculated from gradients of the displacement field, the variation in displacement across a body of typical size L may be estimated to be of the order of $|\Delta u_i| \sim L\,|u_{ij}| \sim LP/E$.

Example 9.1 [Deformation of the legs of a chair]: Standing with your full weight of $M \approx 70$ kg on the seat of a chair supported by four wooden legs with total cross-sectional area $A \approx 30$ cm^2 and $L \approx 50$ cm long, you exert a stress $P \approx Mg_0/A \approx 230$ kPa $= 2.3$ bar on the legs. Taking $E \approx 10^9$ Pa, the deformation will be about $\left|u_{ij}\right| \sim P/E \approx 2.3 \times 10^{-4}$ and the maximal displacement about $|\Delta u_i| \sim PL/E \sim 0.12 \approx$ mm. The squashing of the legs of the chair due to your weight is barely visible.

On the other hand, if gravity is dominant, mechanical equilibrium (9.1a) allows us to estimate the variation in stress over the vertical size L of the body to be $\left|\Delta\sigma_{ij}\right| \approx \rho g L$. The corresponding variation in strain becomes $\left|\Delta u_{ij}\right| \sim L\rho g/E$ for non-exceptional materials. Since u_{ij} is dimensionless, it is convenient to define the *gravitational deformation scale*,

$$D \sim \frac{E}{\rho g}, \tag{9.3}$$

so that $\left|\Delta u_{ij}\right| \sim L/D$. The length D characterizes the scale for major gravitational deformation (of order unity), and small deformations require $L \ll D$. Finally, the gravitationally induced variation in the displacement over a vertical distance L is estimated to be of magnitude $|\Delta u_i| \sim L\left|\Delta u_{ij}\right| \sim L^2/D \ll L$.

Example 9.2 [Gravitational settling of a tall building]: How much does a tall building settle under its own weight when it is built? Let the height of the building be $L = 413$ m, its ground area $A = 63 \times 63$ m^2, and its average mass density one tenth of water, $\rho = 100$ kg m^{-3}, including walls, columns, floors, office equipment and people. The weight of it all is carried by steel columns taking up about $f = 1\%$ of its ground area. The total mass of the building is $M = \rho AL = 1.6 \times 10^8$ kg and the stress in the supports at ground level is $P = Mg_0/fA \approx 400$ bar. Taking Young's modulus to be that of steel, $E = 2 \times 10^{11}$ Pa, the deformation range becomes $\left|\Delta u_{ij}\right| \approx P/E \approx \rho g_0 L/fE$, so that the deformation scale becomes huge, $D \sim fE/\rho g_0 \approx$ 2000 km. The strain range is about 2×10^{-4}, about the same as for the chair, and the top of the building settles by merely $L^2/D \approx 8$ cm.

Saint-Venant's principle

Adhémar Jean Claude Barré de Saint-Venant (1797–1886). French engineer. Worked on mechanics, elasticity, hydrostatics and hydrodynamics. Rederived the Navier–Stokes equations in 1843, avoiding Navier's molecular approach, but did not get credited for these equations with his name. In 1853 he formulated the principle for which he is most remembered.

Suppose an elastic body which is already in mechanical equilibrium is loaded with an additional static force distribution that only acts inside a compact region which is small compared with the general size of the body. The total force as well as the total moment of this distribution must of course vanish, for otherwise the body will not remain in equilibrium. How far will the deformation due to these forces reach? Loosely formulated, Saint-Venant's principle claims that *the deformation due to a localized external force distribution with vanishing total force and total moment of force will decay rapidly and not reach much beyond the linear size of the region of force application*. This is illustrated numerically in figure 9.1 where a pressure distribution with zero total force and total moment is applied to one end of a circular cylinder. One sees that the deformation barely reaches one diameter into the cylinder.

Together with the superposition principle, Saint-Venant's principle is very useful for dealing with the structural statics problems encountered by engineers. It guarantees that the details of how forces are applied locally have essentially no influence on the deformation farther away, as long as the total force and total moment applied in the local region are unchanged. Thus, for example, the difference in floor load when standing with legs together or apart has no consequences for the deformation of the floor except near the place you stand, because your weight is the same and the moment of force vanishes in both positions. Shifting your weight from one foot to the other will on the other hand change the moment of force that you exert on the floor, a moment that must be balanced by an opposite moment from the possibly distant floor supports.

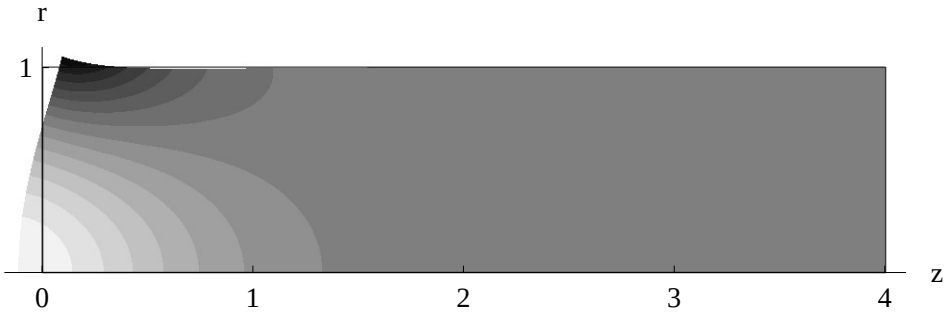

Figure 9.1. Numerical demonstration of Saint-Venant's principle. A circular cylinder with radius $a = 1$ and length $L = 4$ lies with its centerline along the z-axis. You should rotate the figure around the z-axis to see the three-dimensional image. The originally relaxed cylinder is loaded at the left end with a radially varying pressure distribution $p_z = 2r^2 - 1$, for which both the total force and total moment of force vanish. Young's modulus is taken to be 5, and Poisson's ratio 1/3. The gray-levels indicates pressure p_z in the cylinder with black being positive and white negative. The pressure distribution is seen to extend less than one diameter from the left end in accordance with Saint-Venant's principle.

As intuitively right it may appear, Saint-Venant's principle has been difficult to prove in full generality for bodies of all shapes, although mathematical proofs can be found in certain regular geometries [Davis and Selvadurai 1994, IV02, BT08]. Somewhat contrived counterexamples are found in other regular geometries [vM45, Soutas-Little 1999]. The discussion has lasted for 150 years and does not seem to want to end. In the following we shall along with most engineers use the principle to good measure without further worrying about proofs.

9.2 Standing up to gravity

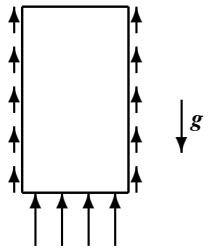

Shear stresses may aid in carrying the weight of a vertical column of elastic material.

Solid objects, be they mountains, bridges, houses or coffee cups, standing on a horizontal surface are deformed by gravity, and deform in turn, by their weight, the supporting surface. Intuition tells us that gravity makes such objects settle towards the ground and squashes their material so that it bulges out horizontally, unless prevented by constraining walls. In a fluid at rest, each horizontal surface element has to carry the weight of the column of fluid above it, and this determines the pressure in the fluid. In a solid at rest, this is more or less also the case, except that shear elastic stresses in the material are able to distribute part or all of the vertical load from the column in the horizontal directions.

Uniform settling

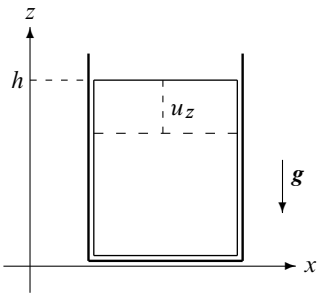

Elastic 'sea' of material undergoing a downwards displacement because of gravity. The container has fixed, slippery walls.

An infinitely extended slab of homogeneous and isotropic elastic material placed on a horizontal surface is a kind of 'elastic sea', which like the fluid sea may be assumed to have the same properties everywhere in a horizontal plane. In a flat-Earth coordinate system, where gravity is given by $\boldsymbol{g} = (0, 0, -g_0)$, we expect a uniformly vertical displacement, which only depends on the z-coordinate,

$$\boldsymbol{u} = (0, 0, u_z(z)) = u_z(z)\,\hat{\boldsymbol{e}}_z. \tag{9.4}$$

In order to realize this "elastic sea" in a finite system, it must be surrounded by fixed, vertical and slippery walls. The vertical walls forbid horizontal but allow vertical displacement, and at the bottom, $z = 0$, we place a horizontal supporting surface which forbids vertical displacement. At the top, $z = h$, the elastic material is left free to move without any external forces acting on it.

The only non-vanishing strain is $u_{zz} = \nabla_z u_z$. From the explicit form of Hooke's law (8.9) , we obtain the non-vanishing stresses

$$\sigma_{xx} = \sigma_{yy} = \lambda u_{zz}, \qquad \sigma_{zz} = (\lambda + 2\mu)u_{zz}, \tag{9.5}$$

and Cauchy's equilibrium equation (9.1a) simplifies in this case to

$$\nabla_z \sigma_{zz} = \rho_0 g_0, \tag{9.6}$$

where ρ_0 is the constant mass density of the undeformed material. Using the boundary condition $\sigma_{zz} = 0$ at $z = h$, this equation may immediately be integrated to

$$\sigma_{zz} = -\rho_0 g_0 (h - z). \tag{9.7}$$

The vertical pressure $p_z = -\sigma_{zz} = \rho_0 g_0 (h - z)$ is positive and rises linearly with depth $h - z$, just as in the fluid sea. It balances everywhere the full weight of the material above, but this was expected since there are no shear stresses to distribute the vertical load. The horizontal pressures $p_x = p_y = p_z \lambda/(\lambda + 2\mu)$ are also positive but smaller than the vertical, because both λ and μ are positive in normal materials. The horizontal pressures are eventually balanced by the stiffness of the fixed vertical walls surrounding the elastic sea.

The strain

$$u_{zz} = \nabla_z u_z = \frac{\sigma_{zz}}{\lambda + 2\mu} = -\frac{\rho_0 g_0}{\lambda + 2\mu}(h - z) \tag{9.8}$$

is negative, corresponding to a compression. The characteristic length scale for major deformation is in this case chosen to be

$$D = \frac{\lambda + 2\mu}{\rho_0 g_0} = \frac{1 - \nu}{(1 + \nu)(1 - 2\nu)} \cdot \frac{E}{\rho_0 g_0}. \tag{9.9}$$

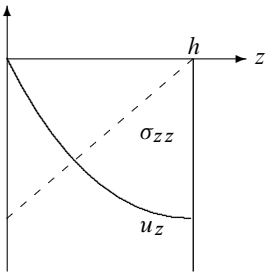

Sketch of the displacement (solid curve) and stress (dashed) for the elastic "elastic sea in a box".

Integrating the strain with the boundary condition $u_z = 0$ for $z = 0$, we finally obtain

$$\boxed{u_z = -\frac{h^2 - (h - z)^2}{2D}.} \tag{9.10}$$

The displacement is always negative, largest in magnitude at the top, $z = h$, and vanishes at the bottom. At the top it varies quadratically with height h, as expected from the estimate in the preceding section.

Shear-free settling

What happens if we remove the vertical container walls around the elastic sea? A fluid would of course spill out all over the place, but an elastic material is only expected to settle a bit more while bulging horizontally out where the walls were before. A cylindrical piece of jelly placed on a flat plate is perhaps the best image to have in mind. In spite of the basic simplicity of the problem, there is no analytic solution to this problem. The numerical solution is shown in figure 9.2.

But if one cannot find the right solution to a problem, it is common practice in physics (as well as in politics) to redefine the problem to fit a solution which one *can* get! What we can obtain is a simple solution with no shear stresses (in the chosen coordinates), but the price we pay is that the vertical displacement will not vanish everywhere at the bottom of the container, as it ought to.

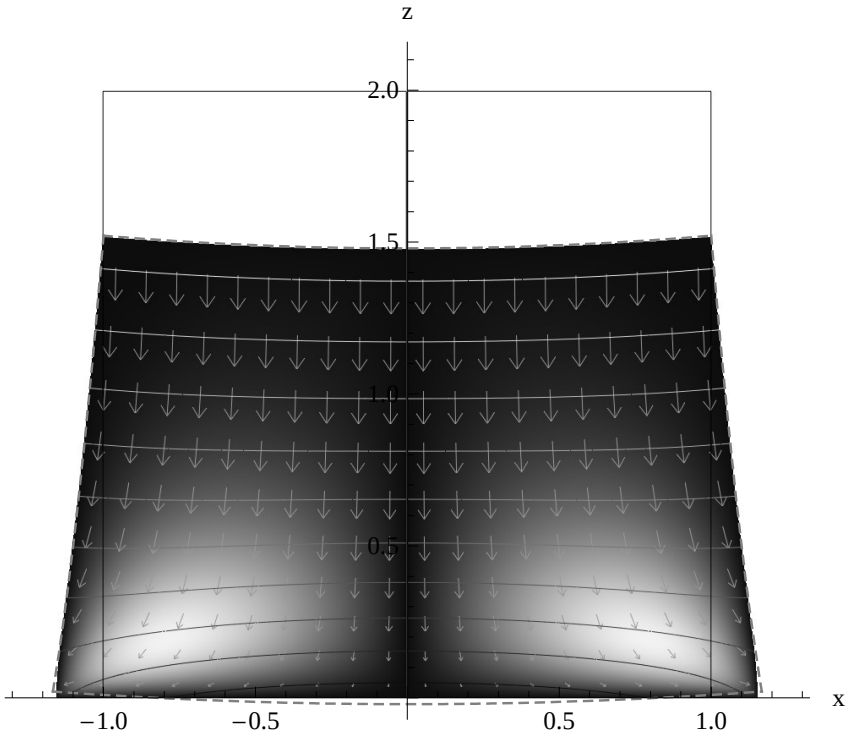

Figure 9.2. Numeric solution to the gravitational settling of a cylindrical block of fairly soft material ("jelly"). The square outline marks the undeformed shape with equal radius $a = 1$ and height $h = 2$, Poisson's ratio $\nu = 1/3$, and deformation scale $D = E/\rho_0 g_0 = 4$. The image is a cut through the xz-plane and should be rotated around the vertical z-axis. The arrows are proportional to the displacement field. The gray-level background indicates shear stress, $\sigma_{rz} = \sigma_{zr}$, with black being low and white high. The fully drawn nearly horizontal lines are isobars for the vertical pressure, showing that it is higher in the middle than at the edges at a given horizontal level. The dashed lines indicate the shape of the deformed block in the shear-free approximation, normalized to vanishing average vertical displacement at $z = 0$. The agreement between model and data is quite impressive.

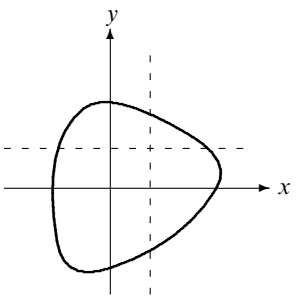

Horizontal cross section of elastic block with vertical sides. Straight lines running parallel with the axes of the coordinate system must cross the outer perimeter in at least two places.

The equilibrium equation (9.1a) with all shear stresses set to zero, i.e. $\sigma_{xy} = \sigma_{yz} = \sigma_{zx} = 0$, now simplifies to

$$\nabla_x \sigma_{xx} = 0, \qquad \nabla_y \sigma_{yy} = 0, \qquad \nabla_z \sigma_{zz} = \rho_0 g_0. \tag{9.11}$$

The first equation says that σ_{xx} does not depend on x, or in other words that σ_{xx} is constant on straight lines parallel with the x-axis. But such lines must always cross the vertical sides, where the x-component of the stress vector, $\sum_j \sigma_{xj} n_j = \sigma_{xx} n_x$, has to vanish, and consequently we must have $\sigma_{xx} = 0$ everywhere. In the same way it follows that $\sigma_{yy} = 0$ everywhere. Finally, the third equation tells us that σ_{zz} is linear in z, and using the condition that $\sigma_{zz} = 0$ for $z = h$ we find

$$\sigma_{zz} = -\rho_0 g_0 (h - z). \tag{9.12}$$

This shows that every column of material carries the weight of the material above it. This result was again to be expected because there are no shear stresses to redistribute the vertical load.

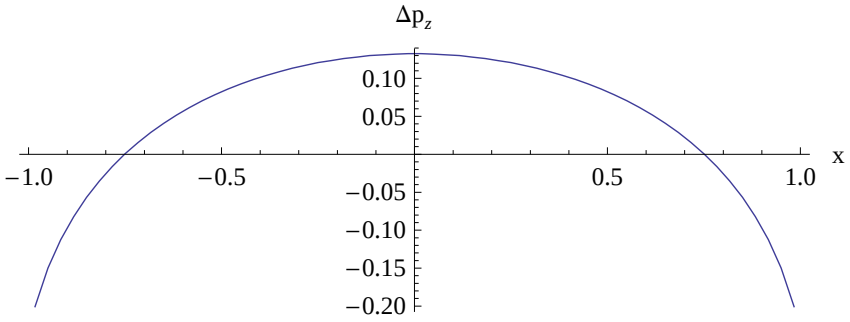

Figure 9.3. The extra vertical pressure distribution at the bottom of a cylindric block, obtained from the numeric solution shown in figure 9.2. The x-coordinate refers to the undeformed body. The total force given by the integral $\mathcal{F}_z = \int_0^1 \Delta p_z(r) 2\pi r\, dr$ vanishes as it should, and the total moment of force vanishes for symmetry reasons.

From the inverse Hooke's law (8.15) , the non-vanishing strain components are,

$$u_{xx} = u_{yy} = \nu \frac{\rho_0 g_0}{E}(h - z), \qquad u_{zz} = -\frac{\rho_0 g_0}{E}(h - z), \tag{9.13}$$

where E is Young's modulus and ν Poisson's ratio. The natural deformation scale is in this case

$$D = \frac{E}{\rho_0 g_0}. \tag{9.14}$$

Using that $u_{xx} = \nabla_x u_x$, and $u_{yy} = \nabla_y u_y$, the horizontal displacements may readily be integrated with boundary conditions $u_x = u_y = 0$ at $x = y = 0$. The integration of $u_{zz} = \nabla_z u_z$ is also straight-forward and leads naively to the same result as for the elastic sea (9.10) , up to an arbitrary function of x and y. This function is determined by the vanishing of the shear stresses u_{xz} and u_{yz}. One may easily verify that the following solution has the desired properties,

$$\boxed{\begin{aligned} u_x &= \nu \frac{(h-z)x}{D}, \\ u_y &= \nu \frac{(h-z)y}{D}, \\ u_z &= -\frac{h^2 - (h-z)^2}{2D} + \nu \frac{x^2 + y^2}{2D} + K. \end{aligned}} \tag{9.15}$$

where K is an arbitrary constant. In any plane parallel with the xy-plane the horizontal displacement represents a uniform expansion with a z-dependent scale factor, which vanishes for $z = h$ and is maximal at $z = 0$.

The trouble with this solution is that we cannot impose the bottom boundary condition, $u_z = 0$ for $z = 0$, for any choice of K. For $K = 0$ the vertical displacement only vanishes at the center $x = y = 0$. Instead of describing the deformation of a block of material resting on a hard and flat horizontal surface, we have obtained a solution which only rests in a single point. For the case of a cylindric block of radius a, the numerical simulation is compared to the shear-free solution in figure 9.2. In this case we have chosen $K = -\nu a^2/4D$, such the integral over the bottom displacement vanishes, $\int_A u_z\, dA = 0$. The block now "rests" on a circle with radius $a/\sqrt{2}$ instead of a point, but also sinks a bit below the surface.

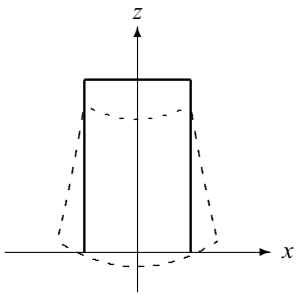

Shear-free model for the gravitational settling of a block of elastic material ("jelly on a plate") in the plane $y = 0$. The model is not capable of fulfilling the boundary condition $u_z = 0$ at $z = 0$ and describes a block which only rests on a circle.

Improving the solution

There can be only one explanation for the failure of the analytic calculation: the initial assumption about the shear-free stress tensor is in conflict with the boundary conditions. What seems to be needed to obtain a solution sitting neatly on a hard, flat supporting surface is an extra vertical pressure distribution from the supporting surface, $z = 0$, which is able to "shore up" the sagging underside of the shear-free solution and make it flat. We cannot solve this problem analytically, but the needed pressure is easily obtained from the simulation and shown in figure 9.3. We also expect that this extra pressure distribution will generate shear stresses, enabling the inner part of the block close to $x = 0$ to carry more than its share of the weight of the material above it, and the outer part near $x = a$ to carry less. This is also seen in the numerical solution in figure 9.2.

For a tall block with height larger than the diameter, Saint-Venant's principle comes to the rescue. The extra pressure exerts vanishing total force on the block because the bottom pressure must carry the weight of the block in both cases, and the total moment of the extra pressure also vanishes for symmetry reasons. The shear-free solution will for this reason be a good approximation to the settling of a tall block, except in a region near the ground comparable to the radius of the block. The simulation in figure 9.2 clearly shows that Saint-Venant's principle holds, even for a cylindrical block with height equal to its diameter.

9.3 Bending a beam

Bending a beam by wrenching it at the ends.

Sticks, rods, girders, struts, masts, towers, planks, poles and pipes are all examples of a generic object, which we shall call a *beam*. Geometrically, a beam consists of a bundle of straight parallel lines or *rays*, covering the same cross section in any plane orthogonal to the lines. Physically, we shall assume that the beam is made from homogeneous and isotropic elastic material.

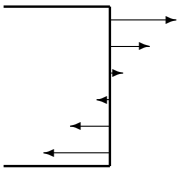

A bending couple may be created by applying normal stresses only to a terminal.

Uniform pure bending

There are many ways to bend a beam. A cantilever is a beam that is fixed at one end and bent like a horizontal flagpole or a fishing rod. A beam may also be supported at the ends and weighed down in the middle like a bridge, but the cleanest way to bend a beam is probably to grab it close to the ends and wrench it like a pencil so that it adopts a uniformly curved shape. Ideally, in *pure bending*, body forces should be absent and external stresses should only be applied to the terminal cross sections. On average these stresses should neither stretch nor compress the beam, but only provide external couples (moments of force) at the terminals. It should be noted that such couples do not require shear stresses, but may be created by normal stresses alone which vary in strength over the terminal cross sections. If you try, you will realize that it is in fact rather hard to bend a pencil in this way. Bending a rubber eraser by pressing it between two fingers is somewhat easier, but tends to add longitudinal compression as well.

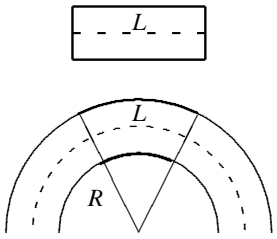

In uniform bending, the bent beam becomes a part of a circular ring.

The bending of the beam is also assumed to be *uniform*, such that the physical conditions, stresses and strains, will be the same everywhere along the beam. This is only possible if the originally straight beam of length L is deformed to become a section of a circular ring of radius R with every ray becoming part of a perfect circle. In that case, it is sufficient to consider just a tiny slice of the beam in order to understand uniform bending for a beam of any length. We shall see later that non-uniform bending can also be handled by piecing together little slices with varying radius of curvature. Furthermore, by appealing to Saint-Venant's principle and linearity, we may even calculate the properties of a beam subject to different types of terminal loads by judicious superposition of displacement fields.

Choice of coordinate system

In a Cartesian coordinate system, we align the undeformed beam with the z-axis, and put the terminal cross sections at $z = 0$ and $z = L$. The length L of the beam may be chosen as small as we please. The cross section A in the xy-plane may be of arbitrary shape, but we may — without loss of generality and for reasons to become clear below — position the coordinate system in the xy-plane with its origin coinciding with the *area centroid* (see eq. (3.16) on page 49), such that the area integral over the coordinates vanishes,

$$\int_A x\, dA = \int_A y\, dA = 0. \tag{9.16}$$

Finally, we require that the central ray after bending becomes part of a circle in the yz-plane with radius R and its center on the y-axis at $y = R$. The radius R is obviously the length scale for major deformation, and must be assumed large compared to the transverse dimensions of the beam.

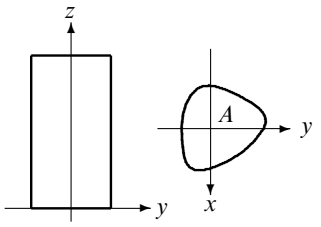

The unbent beam is aligned with the z-axis. Its cross section, A, in the xy-plane is the same for all z.

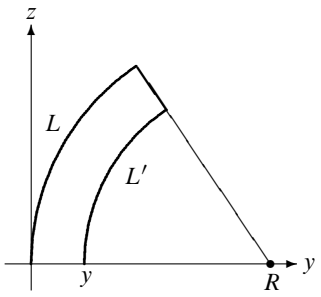

The length of the arc at x must satisfy $L'/(R-y) = L/R$.

Shear-free bending

What precisely happens in the beam when it is bent depends on the way the actual stresses are distributed on its terminals, although by Saint-Venant's principle the details should only matter near the terminals (see figure 9.1). In the simplest case we may view the beam as a loose bundle of thin elastic strings that do not interact with each other, but are stretched or compressed individually according to their position in the beam without generating shear stresses. Let us fix the central string so that it does not change its length L, when bent into a circle of radius R. A simple geometric construction (see the margin figure) then shows that a nearby ray in position x will change its length to L' satisfying $(R-y)/L' = R/L$. Thus according to (7.27) on page 117 the beam experiences a longitudinal strain,

$$u_{zz} = \frac{\delta L}{L} = \frac{L'-L}{L} = -\frac{y}{R}. \tag{9.17}$$

For negative y the material of the beam is being stretched, while for positive y it is being compressed. For the strain to be small, we must have $|y| \ll R$ everywhere in the beam.

Under the assumption that the bending is done without shear and that there are no forces acting on the sides of the beam, it follows as in the preceding section that $\sigma_{xx} = \sigma_{yy} = 0$. The only non-vanishing stress is $\sigma_{zz} = E u_{zz}$, and the non-vanishing strains are as before found from the inverted Hooke's law (8.15) ,

$$u_{xx} = u_{yy} = -\nu u_{zz} = \nu \frac{y}{R}, \tag{9.18}$$

where ν is Poisson's ratio. This shows that the material is being stretched horizontally and compressed vertically for $y > 0$ and conversely for $y < 0$.

Using $u_{ii} = \nabla_i u_i$, and requiring that the central ray, $x = y = 0$, bends a particular solution is found to be

$$\boxed{\begin{aligned} u_x &= \nu \frac{xy}{R}, \\ u_y &= \frac{z^2}{2R} + \nu \frac{y^2 - x^2}{2R}, \\ u_z &= -\frac{yz}{R}. \end{aligned}} \tag{9.19}$$

The second term in u_y is as in the preceding section forced upon us by the requirement of no shear stresses (and strains). For displacement gradients to be small, all dimensions of the beam have to be small compared to R. Note that the beam's actual dimensions do not appear in the displacement field which is therefore a generic solution for pure bending of any beam. For a simple quadratic beam the deformation is sketched in the margin.

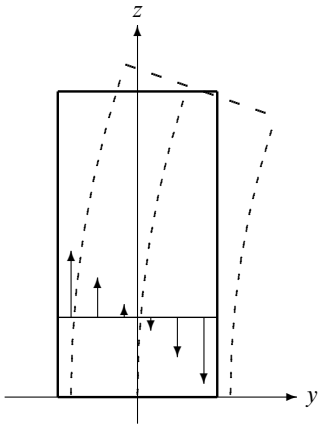

Sketch of the bending of a beam. The arrows show the strain u_{zz}.

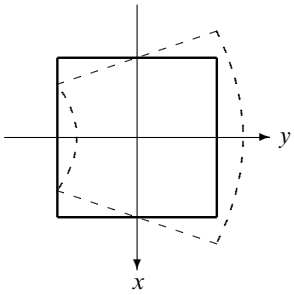

Sketch of the deformation in the xy-plane of a beam with quadratic cross section. This deformation may easily be observed by bending a rubber eraser.

Total force and total moment of force

The only non-vanishing stress component is as mentioned above,

$$\sigma_{zz} = E u_{zz} = -\frac{E}{R} y. \tag{9.20}$$

It is a tension for negative y, and we consequently expect the material of the beam to first break down at the most distant point of the cross section opposite to the direction of bending, as common experience also tells us.

The total force acting on a cross section vanishes

$$\mathcal{F}_z = \int_A \sigma_{zz}\, dS_z = -\frac{E}{R} \int_A y\, dA = 0, \tag{9.21}$$

because the origin of the coordinate system is chosen to coincide with the centroid of the beam cross section (eq. (9.16)).

The moments of the longitudinal stress in any cross section are

$$\mathcal{M}_x = \int_A y\, \sigma_{zz}\, dS_z = -\frac{E}{R} \int_A y^2\, dA, \tag{9.22a}$$

$$\mathcal{M}_y = -\int_A x\, \sigma_{zz}\, dS_z = \frac{E}{R} \int_A xy\, dA, \tag{9.22b}$$

$$\mathcal{M}_z = 0. \tag{9.22c}$$

The component $\mathcal{M}_x$ orthogonal to the bending plane is called the *bending moment*. The integral

$$I = \int_A y^2\, dA \tag{9.23}$$

is the area moment which we have previously introduced on page 51 in connection with ship stability.

The component $\mathcal{M}_y$ vanishes only if,

$$\int_A xy\, dA = 0. \tag{9.24}$$

This will, for example, be the case if the beam has circular cross section, is mirror symmetric under reflection in either axis, or more generally if the axes coincide with the *principal directions* of the cross section. There are always two orthogonal principal directions for any shape of cross section (page 55).

The Euler–Bernoulli law

Liberating ourselves from the coordinate system, we can express the magnitude of the bending moment $\mathcal{M}_b = -\mathcal{M}_x$ in terms of the unsigned radius of curvature R (or curvature $\kappa = 1/R$),

$$\boxed{\mathcal{M}_b = \frac{EI}{R} = EI\kappa.} \tag{9.25}$$

This is the *Euler–Bernoulli law*. The product EI is called the *flexural rigidity* or *bending stiffness* of the beam. The larger it is, the larger is the moment required to bend it with a given radius of curvature. The unit of flexural rigidity is Pa m^4 = N m^2.

The Euler-Bernoulli law is also valid if the beam is subject to *constant* normal or shear stresses in the cross section, because such forces do not contribute to the total moment around the centroid of the cross section. In many engineering applications the Euler–Bernoulli law combined with the superposition principle and Saint-Venant's principle is enough to determine how much a beam is deformed by external loads.

Rectangular beam: A rectangular beam with sides $2a$ and $2b$ along x and y has moment of inertia

$$I = \int_{-a}^{a} dx \int_{-b}^{b} y^2 dy = \frac{4}{3} ab^3. \tag{9.26}$$

It grows more rapidly with the width of the beam in the direction of bending (y) than orthogonally to it (x). This agrees with the common experience that to obtain a given bending radius R it is much easier to bend a beam in the direction where it is thin than in the direction where it is thick.

Elliptic beam: An elliptical beam with major axes $2a$ and $2b$ along x and y has moment of inertia,

$$I = \int_{-a}^{a} dx \int_{-b\sqrt{1-x^2/a^2}}^{b\sqrt{1-x^2/a^2}} y^2\, dy = \frac{4}{3} ab^3 \int_0^1 (1-t^2)^{3/2}\, dt = \frac{\pi}{4} ab^3, \tag{9.27}$$

which is only a little more than half of the rectangular result. An elliptical spring would thus bend about twice the amount of a flat spring of similar dimensions for the same applied moment of force. For a circular beam with radius a, the moment of inertia $I = \frac{\pi}{4}a^4$ is the same in all directions.

Circular pipe: For a circular pipe with inner radius $r = a$ and outer radius $r = b$ we find,

$$I = \int_{a\le r\le b} y^2\, dA = \int_{r\le b} y^2\, dA - \int_{r\le a} y^2\, dA = \frac{\pi}{4}\left(b^4 - a^4\right), \tag{9.28}$$

which (of course) is the difference between the moments of inertia of two circular beams. Due to the fourth power, the moment of inertia and thereby the flexural rigidity is not very dependent on the inner radius (see the margin figure).

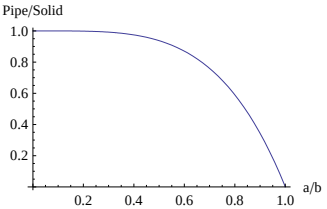

Moment of inertia of a pipe relative to a massive rod of the same outer radius plotted as a function of the ratio of inner and outer radii. The inner radius can be taken as large as $2^{-1/4} = 84\%$ of the outer radius before the moment of inertia is reduced by half.

Example 9.3 [Flexural rigidity of a water pipe]: A one-inch water pipe has inner and outer diameters 2.54 cm and 3.38 cm, implying $I = 4.29$ cm^4. Taking $E = 200$ GPa we get $EI = 8400$ N m^2 which is 2/3 of the flexural rigidity of a massive rod with the same outer radius. It is hard to bend this pipe. If you hang at the end of a one meter long horizontal one-inch pipe with your full weight of 84 kilogram, the radius of curvature becomes 10 meters and the pipe is only bent by about 6 degrees.

Example 9.4 [Flexural rigidity of microtubules]: Microtubules are used for many purposes in the living cell but in particular they provide structural rigidity to the cytoskeleton. They are hollow cylinders made from polymerized protein units arranged in a helical pattern with nearly always 13 such units per turn. Over the years measurements have yielded a large scatter in the flexural rigidities from $1 - 40 \times 10^{-24}$ N m^2 [HCFJ07]. This is now understood as arising from the strong anisotropy in the elastic properties along and around the tubules, preventing pure shear-free bending from being established [PLJ&06].

Yield radius of curvature

As discussed on page 100 the *yield stress* σ_{yield} is defined to be the stress at which a metal becomes ductile and retains its form after a deformation. Using eq. (9.20) with $y = -a$ we obtain the maximal stress Ea/R in a bent circular beam with radius a, so that for the beam to remain elastic, we find the following limits on the radius of curvature and bending moment,

$$R \gtrsim a\frac{E}{\sigma_{\text{yield}}}, \qquad\qquad \mathcal{M}_b \lesssim \frac{\pi}{4} a^3 \sigma_{\text{yield}}. \tag{9.29}$$

The smallest value of R is naturally called the *yield radius of curvature* and the largest value of the bending moment $\mathcal{M}$ the *yield moment*. Interestingly it is independent of Young's modulus.

Example 9.5 [Paperclips]: Anyone who plays with a paperclip during dull board meetings knows that although its purpose requires it to be elastic, it does not take much force to bend it into all kinds of interesting shapes. Paperclips come in many sizes. They are usually made from galvanized steel wire with diameter ranging from 0.5 mm to 2 mm. For steel the typical ratio of Young's modulus to yield stress is about 1000, such that the yield radius for a small paperclip is about 25 cm and for a large 4 times that. The corresponding yield moment for the small clip becomes about 3 N mm, perfect for the kind of light finger manipulation that should not attract much attention. For the large clip with four times the radius of the small, the yield moment is 64 times larger, and attempting to bend the clip into a new shape will hardly go unnoticed by the chairman.

Bending energy

A bent beam contains an elastic energy equal to the work performed by the external forces while bending it. Since the only non-vanishing stress is $\sigma_{zz} = -Ey/R$, it follows immediately from eq. (8.35) on page 136 that the energy density in the beam is $\epsilon = \sigma_{zz}^2/2E = Ey^2/2R^2$. Integrating over the beam cross section we get the total bending energy per unit of beam length,

$$\frac{d\mathcal{E}_b}{d\ell} = \frac{EI}{2R^2} = \frac{\mathcal{M}_b^2}{2EI}, \tag{9.30}$$

where I is the area moment (9.23) . It is of course a constant for pure bending where all cross sections are equivalent, but can also be used for deformations with varying bending moment. We shall return to this in the following chapter.

Extension versus bending

If a beam of length L and cross section area $A \approx a^2$ is subjected to a longitudinal terminal force $\mathcal{F}_z$, its central ray will according to (8.23) on page 133 stretch by $u_z \approx L\mathcal{F}_z/AE$. If it instead is subjected to a transverse terminal force $\mathcal{F}_y$, the central ray will according to (9.19) deflect from a straight line by about $u_y \approx L^2/2R \sim L^3\mathcal{F}_y/EI$, because $\mathcal{M}_b \sim L\mathcal{F}_y$ at $z \approx 0$. Since $I \sim Aa^2$, the ratio of longitudinal to transverse displacement becomes

$$\left|\frac{u_z}{u_y}\right| \sim \frac{a^2}{L^2}\left|\frac{\mathcal{F}_z}{\mathcal{F}_y}\right|. \tag{9.31}$$

This shows that for thin beams with $a \ll L$, and comparable longitudinal and transverse forces, $\left|\mathcal{F}_z/\mathcal{F}_y\right| \approx 1$, the longitudinal displacement is always negligible relative to the transverse.

9.4 Twisting a shaft

The drive shaft in older cars and in trucks connects the gear box to the differential and transmits engine power to the rear wheels. In characterizing engine performance, maximum torque is often quoted, because it creates the largest shear force between wheels and road and therefore maximal acceleration, barring wheel-spin. Although the shaft is made from steel, it will nevertheless undergo a tiny deformation in the form of a *torsion* or *twist*.

Pure torsion

Let the shaft be a beam with circular cross section of radius a and axis coinciding with the z-axis[1]. The deformation is said to be a *pure torsion* if the shaft's material is rotated by a constant amount τ per unit of length, such that a given cross section at the position z is rotated by an angle τz relative to the cross section at $z = 0$. The constant τ which measures the rotation angle per unit of length of the beam is called the *torsion*. Its inverse, $1/\tau$, is the length of a beam that undergoes a pure torsion through one radian. It could be called the *torsion length*, although this is not commonly used. It is analogous to the radius of curvature $R = 1/\kappa$ for pure bending which is the length of a beam that is bent through one radian.

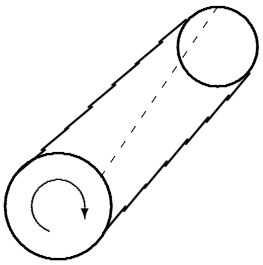

Pure torsion consists of rotating every cross section by a fixed amount per unit of length.

The uniform nature of pure torsion allows us to consider just a small slice of the shaft of length L which is only twisted through a tiny angle, $\tau L \ll 1$. Since the physical conditions are the same in all such slices, we can later put them together to make a shaft of any length. To lowest order in the vector angle $\boldsymbol{\phi} = \tau z \hat{\boldsymbol{e}}_z$, the displacement field in the slice becomes,

$$\boldsymbol{u} = \boldsymbol{\phi} \times \boldsymbol{x} = \tau z \hat{\boldsymbol{e}}_z \times \boldsymbol{x} = \tau z(-y, x, 0). \tag{9.32}$$

Not surprisingly, it is purely tangential and is always much smaller than the radius of the shaft, $|\boldsymbol{u}| = \tau\,|z|\,|\boldsymbol{x}| \leq \tau L a \ll a$, because $\tau L \ll 1$.

Strains and stresses

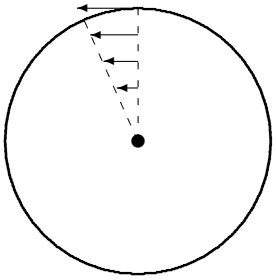

The displacement field for a rotation through a tiny angle τz (exaggerated here) is purely tangential and grows linearly with the radial distance.

The displacement gradient tensor becomes

$$\{\nabla_j u_i\} = \begin{pmatrix} 0 & -\tau z & -\tau y \\ \tau z & 0 & \tau x \\ 0 & 0 & 0 \end{pmatrix}, \tag{9.33}$$

and for this matrix to be small, we must also require $\tau a \ll 1$, or in other words that the twist must be small over a length of the shaft comparable to its radius. The only non-vanishing strains are,

$$u_{xz} = u_{zx} = -\tfrac{1}{2}\tau y, \qquad u_{yz} = u_{zy} = \tfrac{1}{2}\tau x, \tag{9.34}$$

and the corresponding stresses are obtained from the isotropic Hooke's law (8.8) on page 128,

$$\sigma_{xz} = \sigma_{zx} = -\mu\tau y, \qquad \sigma_{yz} = \sigma_{zy} = \mu\tau x. \tag{9.35}$$

Inserting these stresses into the equilibrium equation (9.1a) , it is seen that it is trivially fulfilled. On vector form these equations may be written

$$\boldsymbol{\sigma} \cdot \hat{\boldsymbol{e}}_r = \boldsymbol{0}, \qquad \boldsymbol{\sigma} \cdot \hat{\boldsymbol{e}}_z = \mu\tau \hat{\boldsymbol{e}}_z \times \boldsymbol{x} \tag{9.36}$$

where $\hat{\boldsymbol{e}}_r = (x, y, 0)/r$ is the radial unit vector (and $r = \sqrt{x^2 + y^2}$). The first of these equations shows that on the cylindrical surface of the shaft, the stress vector vanishes, as it should when there are no external forces acting there.

In order to realize a pure torsion, the correct stress distribution (9.36) must be applied to the ends of the shaft. Applying a different stress distribution, for example by grabbing both ends of the shaft with monkey-wrenches and twisting, leads to a different solution near the end, but the pure torsion solution should according to Saint-Venant's principle still be valid everywhere, except within one diameter from the ends.

[1]The solution for circular cross section was first obtained by Coulomb in 1787, whereas the more complicated case of beams with non-circular cross section was analyzed by Saint-Venant in 1855 (see [Landau and Lifshitz 1986, p. 59] or [Sokolnikoff 1956, p. 109]). There is in fact no explicit solution in the general non-circular case.

The Coulomb-Saint-Venant law

In any cross section we may calculate the total moment of force around the shaft axis, in this context called the *torque*. On a surface element $d\boldsymbol{S}$, the moment is $d\boldsymbol{\mathcal{M}} = \boldsymbol{x} \times d\boldsymbol{\mathcal{F}} = \boldsymbol{x} \times \boldsymbol{\sigma} \cdot d\boldsymbol{S}$. Since the cross section lies in the xy-plane, the z-component of the torque becomes,

$$\mathcal{M}_z = \int_A (x\sigma_{yz} - y\sigma_{xz})\, dA = \mu\tau \int_A (x^2 + y^2) dxdy. \tag{9.37}$$

Liberating ourselves from the coordinate system, the torque $M_t = M_z$ can always be written analogously to the Euler-Bernoulli law (9.25) ,

$$\boxed{\mathcal{M}_t = \mu J\, \tau} \tag{9.38}$$

where J for a circular pipe with inner and outer radii, a and b, becomes,

$$J = \int_{a \le r \le b} (x^2 + y^2) dxdy = \frac{\pi}{2}\left(b^4 - a^4\right). \tag{9.39}$$

For non-circular cross sections the result may be found in [Landau and Lifshitz 1986, p. 62].

The quantity μJ is called the *torsional rigidity* of the beam. For a pipe with circular cross section we have $J = 2I$, implying that $EI = (1+\nu)\mu J$, where ν is Poisson's ratio. Knowing the torsional rigidity and the torque $\mathcal{M}_t$, one may calculate the torsion, $\tau = \mathcal{M}_z/\mu J$ and conversely. Like the flexural rigidity, the torsional rigidity grows rapidly with the radius of the beam, and pipes with walls that are not too thin have also nearly the same torsional rigidity as a massive rod.

Transmitted power

If the shaft rotates with constant angular velocity Ω, the material at the point (x, y, z) will have velocity $\boldsymbol{v}(x, y) = \Omega\hat{\boldsymbol{e}}_z \times \boldsymbol{x} = \Omega(-y, x, 0)$. The shear stresses acting on an element of the cross section, $d\boldsymbol{S} = \hat{\boldsymbol{e}}_z dxdy$, will transmit a *power* (i.e. work per unit of time) of $dP = \boldsymbol{v} \cdot d\boldsymbol{\mathcal{F}} = \boldsymbol{v} \cdot \boldsymbol{\sigma} \cdot d\boldsymbol{S}$ to the shaft. Integrating over the cross section the total power becomes,

$$P = \int_A \boldsymbol{v} \cdot \boldsymbol{\sigma} \cdot d\boldsymbol{S} = \int_A \Omega(x\sigma_{yz} - y\sigma_{xz}) dxdy = \Omega\mathcal{M}_z = \boldsymbol{\Omega} \cdot \boldsymbol{\mathcal{M}}. \tag{9.40}$$

As the derivation shows, this relation does not depend on the actual stress distribution, but is generally valid for the instantaneous power delivered by the torque $\boldsymbol{\mathcal{M}}$ acting on a body rotating with angular velocity vector $\boldsymbol{\Omega}$.

Example 9.6 [Car engine]: The typical torque delivered by a family car engine can be of the order of 100 Nm. If the shaft rotates with 3000 rpm, corresponding to an angular velocity of $\Omega \approx 314\ \mathrm{s}^{-1}$, the transmitted power is about 31.4 kW, or 42 horsepower. For a drive shaft made of steel with radius $a = 2$ cm, the torsional rigidity is $C \approx 2 \times 10^4\ \mathrm{Nm}^2$. In direct drive without gearing, the torsion becomes $\tau \approx 0.005\ \mathrm{m}^{-1} = 0.3^\circ\ \mathrm{m}^{-1}$. For a car with rear-wheel drive, the length of the drive shaft may be about 2 m, and the total twist amounts to about 0.6°. The maximal shear stress in the material is $\mu\tau a \approx 8 \times 10^6$ Pa $= 80$ bar at the rim of the shaft.

Torsion energy

A twisted beam contains elastic energy, just like a bent beam. Since there are only four stress components that are non-vanishing we find from the energy density (8.35) on page 136 that the torsional energy per unit of beam length is

$$\frac{d\mathcal{E}_t}{d\ell} = \frac{1}{2}\mu J \tau^2 = \frac{\mathcal{M}_t^2}{2\mu J}. \tag{9.41}$$

It is of course constant for pure torsion where all cross sections are equivalent, but may also be used for deformations with varying torque.

* 9.5 Radial deformation of spherical body

A spherically shaped vessel withstands external pressure better than any other shape and has for that reason been used for extreme deep sea exploration. Intuitively this is clear from symmetry alone. Since the water pressure is the same in all directions, the spherical shape ought to be the one that best withstands collapse, because the collapse — so to speak — can find no place to begin. Nevertheless, in films of deep-sea diving, you see the rivets beginning to pop on the inside of the vessel. Why is that?

Uniform radial displacement

Spheres can be deformed in an infinity of different ways, but we shall in the following analysis only consider radial displacement fields of the form

$$\boldsymbol{u} = u_r(r)\,\hat{\boldsymbol{e}}_r \tag{9.42}$$

where $\hat{\boldsymbol{e}}_r = \boldsymbol{x}/r$ is the radial unit vector in coordinates with origin in the center of the sphere. Note that we keep the redundant index r to remind us that this is the radial component. At this point we could introduce full-fledged spherical coordinates (see appendix D), but the simplicity of the radial field allows us to open a bag of tricks that makes it unnecessary.

Equilibrium equation

Using that the radial unit vector is the gradient or the radial coordinate, $\hat{\boldsymbol{e}}_r = \nabla r$, we can write the uniform radial displacement as the gradient of a helper field $\psi(r)$,

$$\boldsymbol{u} = u_r\hat{\boldsymbol{e}}_r = \frac{d\psi}{dr}\nabla r = \nabla\psi(r), \qquad \psi(r) = \int u_r(r)\,dr. \tag{9.43}$$

A short calculation shows that the Laplacian of the displacement field becomes itself a gradient,

$$\nabla^2\boldsymbol{u} = \nabla^2\nabla\psi = \nabla\nabla^2\psi = \nabla\nabla\cdot\nabla\psi = \nabla\nabla\cdot\boldsymbol{u}$$

so that the Navier–Cauchy equation (9.2) takes the much simpler form

$$(2\mu+\lambda)\nabla\nabla\cdot\boldsymbol{u} = -\boldsymbol{f}\,. \tag{9.44}$$

Since $\nabla\cdot\boldsymbol{u}$ can only depend on r for symmetry reasons, it follows that the only body force consistent with the radial assumption must itself be radial, $\boldsymbol{f} = f_r(r)\hat{\boldsymbol{e}}_r$.

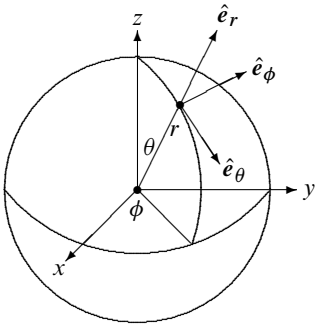

Spherical coordinates with radial basis vector $\hat{\boldsymbol{e}}_r$ and tangential basis vectors $\hat{\boldsymbol{e}}_\theta$ and $\hat{\boldsymbol{e}}_\phi$.

Gauss theorem leads to the following identity for the volume integral over the sphere,

$$4\pi r^2 u_r = \oint_S \boldsymbol{u} \cdot d\boldsymbol{S} = \int_V \boldsymbol{\nabla} \cdot \boldsymbol{u}\, dV = \int_0^r \boldsymbol{\nabla} \cdot \boldsymbol{u}\, 4\pi r^2 dr. \tag{9.45}$$

Differentiating both sides with respect to r we get

$$\boldsymbol{\nabla} \cdot \boldsymbol{u} = \frac{1}{r^2}\frac{d(r^2 u_r)}{dr}, \tag{9.46}$$

so that the Navier-Cauchy equation reduces to a second-order ordinary differential equation,

$$\boxed{\frac{d}{dr}\left(\frac{1}{r^2}\frac{d(r^2 u_r)}{dr}\right) = -f_r\ ,} \tag{9.47}$$

The only radial body force that naturally could come into play is of course gravity in a solid planet, for example the Moon.

Strains and stresses

Using dyadic notation, the displacement gradients are simple to evaluate,

$$\boldsymbol{\nabla u} = \boldsymbol{\nabla}\left(\frac{u_r}{r}\boldsymbol{x}\right) = \boldsymbol{\nabla}\left(\frac{u_r}{r}\right)\boldsymbol{x} + \frac{u_r}{r}\mathbf{1} = \frac{du_r}{dr}\hat{\boldsymbol{e}}_r\hat{\boldsymbol{e}}_r + \frac{u_r}{r}(\mathbf{1} - \hat{\boldsymbol{e}}_r\hat{\boldsymbol{e}}_r). \tag{9.48}$$

It is obviously symmetric, and thus equal to the strain tensor, $\boldsymbol{u} = \boldsymbol{\nabla u}$. The only non-vanishing components of the strain tensor are its projections on the radial and tangential directions,

$$u_{rr} = \hat{\boldsymbol{e}}_r \cdot \boldsymbol{u} \cdot \hat{\boldsymbol{e}}_r = \frac{du_r}{dr}, \qquad u_{tt} = \hat{\boldsymbol{e}}_t \cdot \boldsymbol{u} \cdot \hat{\boldsymbol{e}}_t = \frac{u_r}{r} \tag{9.49}$$

where $\hat{\boldsymbol{e}}_t$ is any tangential unit vector orthogonal to $\hat{\boldsymbol{e}}_r$.

Choosing any two orthogonal tangential directions, the non-vanishing components of the stress tensor become

$$\sigma_{rr} = 2\mu u_{rr} + \lambda(u_{rr} + 2u_{tt}), \qquad \sigma_{tt} = 2\mu u_{tt} + \lambda(u_{rr} + 2u_{tt}). \tag{9.50}$$

Notice that the coefficient of λ equals the divergence (9.46) , as it should.

Spherical shell under external pressure

In the absence of gravity, $f_r = 0$, the most general solution is easily found from eq. (9.47) ,

$$u_r = Ar + \frac{B}{r^2}, \tag{9.51}$$

where A and B are integration constants. The strains and stresses become

$$u_{rr} = A - \frac{2B}{r^3}, \qquad u_{tt} = A + \frac{B}{r^3} \tag{9.52}$$

$$\sigma_{rr} = (2\mu + 3\lambda)A - 4\mu\frac{B}{r^3}, \qquad \sigma_{tt} = (2\mu + 3\lambda)A + 2\mu\frac{B}{r^3}. \tag{9.53}$$

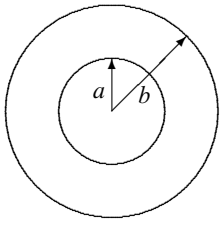

A spherical shell with inner radius a and outer radius b.

Let the spherical shell have inner and outer radii a and b. The boundary conditions are now $\sigma_{rr} = 0$ for $r = a$ and $\sigma_{rr} = -P$ for $r = b > a$ (corresponding to a positive external pressure P), leading to two linear equations for A and B. The solution is,

$$A = -\frac{b^3}{b^2 - a^3}\frac{P}{2\mu + 3\lambda}, \qquad B = -\frac{a^3 b^3}{b^3 - a^3}\frac{P}{4\mu}. \tag{9.54}$$

Notice that both integration constants are negative.

Displacement: Expressed in terms of Young's modulus E and Poisson's ratio ν, the displacement becomes

$$\boxed{u_r = -\frac{b^3}{b^3 - a^3}\left((1-2\nu)r + (1+\nu)\frac{a^3}{2r^2}\right)\frac{P}{E}} \tag{9.55}$$

which is always negative, as we would expect under a compression.

From the displacement we may calculate the change in thickness $d = b - a$,

$$\delta d = u_r(b) - u_r(a) = -\frac{b^3}{b^2 + ab + a^2}\left(1 - 2\nu - (1+\nu)\frac{a(a+b)}{2b^2}\right)\frac{P}{E} \tag{9.56}$$

Surprisingly, for a range of values of b/a including $b/a = 1$, the parenthesis is negative, such that the shell actually *thickens* when compressed (see problem 9.9). A similar result holds for a cylindrical tube (problem 9.5). This is probably why you see rivets jumping out of the hull in films of submarines going too deep, because they are literally being pulled out by the increase of the wall thickness caused by compression.

Strains: The strains become

$$u_{rr} = -\frac{b^3}{b^3 - a^3}\left(1 - 2\nu - (1+\nu)\frac{a^3}{r^3}\right)\frac{P}{E}, \tag{9.57a}$$

$$u_{tt} = -\frac{b^3}{b^3 - a^3}\left(1 - 2\nu + (1+\nu)\frac{a^3}{2r^3}\right)\frac{P}{E}. \tag{9.57b}$$

Since $-1 < \nu < 1/2$, the tangential strain u_{tt} is always negative, corresponding to a tangential compression of the material. The radial strain u_{rr} is always positive at the inside of the shell at $r = a$, and can even be positive at the outside $r = b$. This is of course related to the thickening of the shell. Although the material is everywhere displaced radially inwards, it will always expand at the inside for $r = a$, but may expand or contract at the outside.

Stresses: The stresses become

$$\sigma_{rr} = -\frac{b^3}{b^3 - a^3}\left(1 - \frac{a^3}{r^3}\right)P, \tag{9.58a}$$

$$\sigma_{tt} = -\frac{b^3}{b^3 - a^3}\left(1 + \frac{a^3}{2r^3}\right)P. \tag{9.58b}$$

Again there is surprise: The stresses are independent of the elastic properties of the material.

Example 9.7 [The bathysphere]: The first deep-sea vessel, the bathysphere, was spherical and tethered to a surface vessel. It reached a record depth of 923 meter in 1932 with two pilots in its tiny chamber. It was made from cast steel with inner diameter $2a = 4.75$ ft $= 145$ cm and thickness $d = 1$ in $= 2.54$ cm. Since $d/a \approx 0.035$ it is appropriate to use the thin shell formulas. Taking $P = 100$ bar, $E = 200$ GPa and $\nu = 1/3$ we find $u_r \approx -0.35$ mm, $\delta d \approx 12$ μm, $u_{rr} = -u_{tt} = \approx 5 \times 10^{-4}$, and an impressive tangential stress, $\sigma_{tt} \approx -1400$ Bar. This is not far the tensile strength of steel, which is about 2000-4000 Bar, although the compressive strength may be a factor 10 larger than that.

Example 9.8 [The bathyscaphe]: The tethering of the bathysphere to a surface vessel limited the depth that could be reached by this construction. Instead a self-contained dirigible deep-sea vessel, called the bathyscaphe by its inventor Auguste Picard, was constructed in the late 1940s. A second version, named the *Trieste*, was built and launched in 1953 (see figure 9.4). Most of the

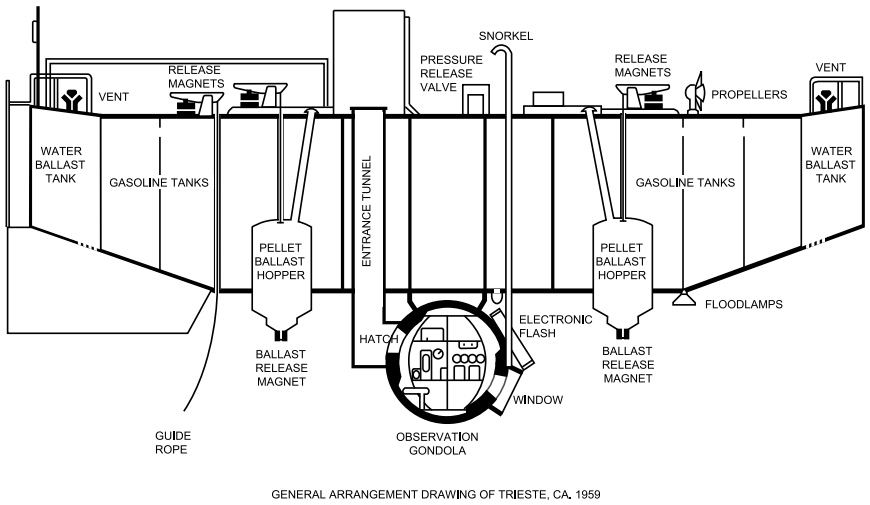

Figure 9.4. Sketch of the structure of the bathyscaphe Trieste which reached the bottom of the nearly 11,000 meter deep Challenger Deep in the Mariana Trench on January 23, 1960. The physical properties of the spherical crew cabin are discussed in example 9.8. Figure redrawn by Ralph Sutherland (2007) from U.S. Naval Historical Center Photograph NH96807. Reproduced here under Wikimedia Commons license.

vessel was cylindrical and with open floatation tanks containing gasoline (for buoyancy) and other equipment that did not have to withstand enormous pressure differences. The crew chamber was as before a sphere, this time with a diameter of $2a = 200$ cm and thickness $d = 5$ in $= 12.7$ cm. Since $d/a = 0.127$, we use the exact formulas and find with the same material parameters as above that $u_r \approx -1.8$ mm, $\delta d \approx 0.18$ mm, and $\sigma_{tt} \approx -4300$ Bar. The sphere was carefully constructed by the German Krupp Steel Works to avoid potentially deadly weaknesses in its hull and observation ports. It reached the ultimate depth on Earth, the nearly 11 kilometer Challenger Deep of the Mariana Trench, on January 23 1960, a feat yet to be repeated.

Thin shell

For a thin shell we expand to leading order in the thickness $d = b - a$ and get for $d \ll a$,

$$u_r \approx -(1-\nu)\frac{a^2}{2d}\frac{P}{E}, \qquad \delta d \approx \nu a \frac{P}{E}, \tag{9.59}$$

$$u_{rr} \approx \nu \frac{a}{d}\frac{P}{E}, \qquad u_{tt} \approx -\frac{1}{2}(1-\nu)\frac{a}{d}\frac{P}{E} \tag{9.60}$$

$$\sigma_{rr} \approx -sP, \qquad \sigma_{tt} \approx -\frac{1}{2}\frac{a}{d}P \tag{9.61}$$

where the variable $s = (r-a)/(b-a)$ ranges between 0 and 1. Again we note that the shell thickens, and that there is radial expansion and tangential compression for $\nu > 0$. The tangential stress is greater than the applied pressure by a large factor $a/2d$.

* 9.6 Radial deformation of cylindrical body

Cylindrical pipes (or tubes) carrying fluids under pressure are found everywhere, in living organisms and in machines, not forgetting the short moments of intense pressure in the barrel of a gun or canon. How much does a pipe expand under pressure, and how is the deformation distributed? What are the stresses in the material and where will it tend to break down?

Uniform radial displacement

The ideal pipe is a right circular cylinder with inner radius a, outer radius b and length L, made from homogeneous and isotropic elastic material. When subjected to a uniform internal pressure, the pipe is expected to expand radially and perhaps also contract longitudinally. We shall to begin with prevent the contraction by clamping the ends of the pipe such that its length remains unchanged while it exerts a negative pressure on the clamps.

Under these assumptions, the only freedom for the pipe is to expand radially and uniformly such that the displacement fields takes the form,

$$\boldsymbol{u} = u_r(r)\,\hat{\boldsymbol{e}}_r, \tag{9.62}$$

where $u_r(r)$ is only a function of the axial distance $r = \sqrt{x^2 + y^2}$. The three unit vectors (see the margin figure),

$$\hat{\boldsymbol{e}}_r = \frac{(x, y, 0)}{r}, \qquad \hat{\boldsymbol{e}}_\phi = \frac{(-y, x, 0)}{r}, \qquad \hat{\boldsymbol{e}}_z = (0, 0, 1), \tag{9.63}$$

form a local basis for any cylindrical geometry (see appendix D). The following analysis proceeds roughly along the same path as in the preceding section with some repetition.

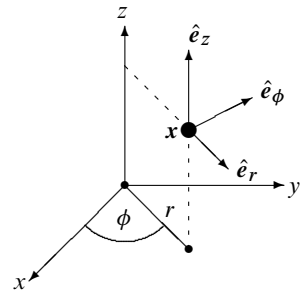

Cylindrical coordinates and basis vectors (see appendix D).

Equilibrium equation

Since $\nabla r = \hat{\boldsymbol{e}}_r$, it follows from the radial assumption (9.62) that the displacement field may be written as the gradient of another field,

$$\boldsymbol{u} = u_r \hat{\boldsymbol{e}}_r = \frac{d\psi}{dr}\nabla r = \nabla\psi(r), \qquad \psi(r) = \int u_r(r)\,dr. \tag{9.64}$$

The Laplacian of the displacement field can now be written as a gradient, $\nabla^2\boldsymbol{u} = \nabla^2\nabla\psi = \nabla\nabla^2\psi = \nabla\nabla\cdot\boldsymbol{u}$, so that the Navier–Cauchy equation (9.2) takes the much simpler form

$$(2\mu + \lambda)\,\nabla\nabla\cdot\boldsymbol{u} = -\boldsymbol{f}\,. \tag{9.65}$$

Cylindrical symmetry demands that $\nabla\cdot\boldsymbol{u}$ can only depend on r, and thus that the body force density, if present, must also be radial, $\boldsymbol{f} = f_r(r)\hat{\boldsymbol{e}}_r$.

Using again that the divergence only depends on r, and Gauss' theorem, we obtain the following identity for the volume integral over a piece of the cylinder of length L,

$$2\pi r L u_r = \oint_S \boldsymbol{u}\cdot d\boldsymbol{S} = \int_V \nabla\cdot\boldsymbol{u}\,dV = \int_0^r \nabla\cdot\boldsymbol{u}\,2\pi r L dr. \tag{9.66}$$

Differentiating both sides with respect to r we get

$$\nabla\cdot\boldsymbol{u} = \frac{1}{r}\frac{d(ru_r)}{dr}, \tag{9.67}$$

and finally we arrive at the ordinary second-order differential equation in r,

$$\boxed{(\lambda + 2\mu)\,\frac{d}{dr}\left(\frac{1}{r}\frac{d(ru_r)}{dr}\right) = -f_r,} \tag{9.68}$$

which may be integrated with suitable boundary conditions to yield the radial displacement. The only natural candidate for a radial body force is the centrifugal force on a cylinder rotating around its axis.

Strains and stresses

The displacement gradients are most easily calculated in Cartesian coordinates, where

$$u_x = x\frac{u_r}{r}, \qquad u_y = y\frac{u_r}{r}. \tag{9.69}$$

Using that $\nabla_x r = x/r$ and $\nabla_y r = y/r$, the non-vanishing displacement gradients become,

$$\begin{aligned}
\nabla_x u_x &= \frac{u_r}{r} + \frac{x^2}{r}\frac{d(u_r/r)}{dr} = \frac{x^2}{r^2}\frac{du_r}{dr} + \frac{y^2}{r^2}\frac{u_r}{r},\\
\nabla_y u_y &= \frac{u_r}{r} + \frac{y^2}{r}\frac{d(u_r/r)}{dr} = \frac{y^2}{r^2}\frac{du_r}{dr} + \frac{x^2}{r^2}\frac{u_r}{r},,\\
\nabla_x u_y &= \nabla_y u_x = \frac{xy}{r}\frac{d(u_r/r)}{dr} = \frac{xy}{r^2}\frac{du_r}{dr} - \frac{xy}{r^2}\frac{u_r}{r}.
\end{aligned}$$

Expressed in dyadic notation (see page 599), the displacement gradients may be compactly written

$$\boldsymbol{\nabla u} = \frac{du_r}{dr}\hat{\boldsymbol{e}}_r\hat{\boldsymbol{e}}_r + \frac{u_r}{r}\hat{\boldsymbol{e}}_\phi\hat{\boldsymbol{e}}_\phi. \tag{9.70}$$

The right-hand side is a symmetric matrix and thus identical to Cauchy's strain tensor $\boldsymbol{u}$. We note that the trace of this matrix equals $\boldsymbol{\nabla}\cdot\boldsymbol{u}$, as it should.

The only non-vanishing components of the strain tensor are

$$u_{rr} = \frac{du_r}{dr}, \qquad u_{\phi\phi} = \frac{u_r}{r}. \tag{9.71}$$

The non-vanishing stress tensor components are found from Hooke's law (8.8) by projecting on the basis vectors

$$\sigma_{rr} = 2\mu u_{rr} + \lambda\left(u_{rr} + u_{\phi\phi}\right), \tag{9.72a}$$
$$\sigma_{\phi\phi} = 2\mu u_{\phi\phi} + \lambda\left(u_{rr} + u_{\phi\phi}\right), \tag{9.72b}$$
$$\sigma_{zz} = \lambda\left(u_{rr} + u_{\phi\phi}\right). \tag{9.72c}$$

Here we have used that the trace of the strain tensor is independent of the basis, so that $\sum_k u_{kk} = u_{xx} + u_{yy} = u_{rr} + u_{\phi\phi}$. The longitudinal stress, σ_{zz}, appears as a consequence of the clamping of the ends of the cylinder.

Clamped pipe under internal pressure

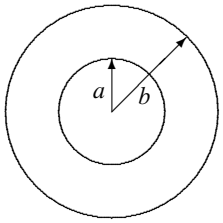

Cylindrical pipe with inner radius a and outer radius b.

In the simplest case there are no body forces, $f_r = 0$, and we find immediately the solution

$$u_r = Ar + \frac{B}{r}, \tag{9.73}$$

where A and B are integration constants to be determined by the boundary conditions. The strains and stresses become

$$u_{rr} = A - \frac{B}{r^2}, \qquad u_{\phi\phi} = A + \frac{B}{r^2}, \tag{9.74}$$

$$\sigma_{rr} = 2A\left(\lambda+\mu\right) - \frac{2\mu B}{r^2}, \qquad \sigma_{\phi\phi} = 2A\left(\lambda+\mu\right) + \frac{2\mu B}{r^2}, \qquad \sigma_{zz} = 2A\lambda. \tag{9.75}$$

The boundary conditions are $\sigma_{rr} = -P$ at the inside surface $r = a$ and $\sigma_{rr} = 0$ at the outside surface $r = b$. The minus sign may be a bit surprising, but remember that the normal to the

inside surface of the pipe is in the direction of $-\hat{\boldsymbol{e}}_r$, so that the stress vector $\sigma_{rr}(-\hat{\boldsymbol{e}}_r) = P\hat{\boldsymbol{e}}_r$ points in the positive radial direction, as it should. The boundary conditions are solved for A and B, and we find,

$$A = \frac{a^2}{b^2-a^2}\frac{P}{2(\lambda+\mu)}, \qquad B = \frac{a^2b^2}{b^2-a^2}\frac{P}{2\mu}. \tag{9.76a}$$

Note that both are positive.

Displacement field: Expressed in terms of Young's modulus E and Poisson's ratio ν, the radial displacement field becomes

$$u_r = (1+\nu)\frac{a^2}{b^2-a^2}\left((1-2\nu)r + \frac{b^2}{r}\right)\frac{P}{E}. \tag{9.77}$$

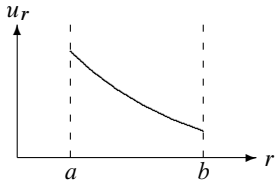

Sketch of the displacement field.

Since $\nu \leq 1/2$, the radial displacement field is always positive and monotonically decreasing for $a \leq r \leq b$. It reaches its maximum at the inner surface, $r = a$, confirming the intuition that the pressure in the pipe should push the innermost material farthest away from its original position.

Strain tensor: The non-vanishing strain tensor components become

$$u_{rr} = (1+\nu)\frac{a^2}{b^2-a^2}\left(1-2\nu-\frac{b^2}{r^2}\right)\frac{P}{E}, \tag{9.78a}$$

$$u_{\phi\phi} = (1+\nu)\frac{a^2}{b^2-a^2}\left(1-2\nu+\frac{b^2}{r^2}\right)\frac{P}{E}. \tag{9.78b}$$

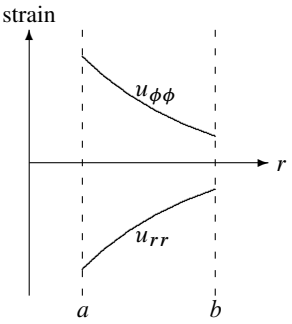

Sketch of strain components.

For normal materials with $0 < \nu \leq 1/2$, the radial strain u_{rr} is negative, corresponding to a compression of the material, whereas the tangential strain $u_{\phi\phi}$ is always positive, corresponding to an extension. There is no longitudinal strain because of the clamping of the ends of the pipe.

The scale of the strain is again set by the ratio P/E. For normal materials under normal pressures, for example an iron pipe with $E \approx 1$ Mbar subject to a water pressure of a few bars, the strain is only of the order of parts per million, whereas the strains in the walls of your garden hose or the arteries in your body are much larger. When the walls become thin, i.e. for $d = b-a \ll a$, the strains grow stronger because of the denominator $b^2-a^2 \approx 2da$, and actually diverge towards infinity in the limit. This is in complete agreement with our understanding that the walls of a pipe need to be of a certain thickness to withstand the internal pressure.

Stress tensor: The non-vanishing stress tensor components become

$$\sigma_{rr} = -\frac{a^2}{b^2-a^2}\left(\frac{b^2}{r^2}-1\right)P, \tag{9.79a}$$

$$\sigma_{\phi\phi} = \frac{a^2}{b^2-a^2}\left(\frac{b^2}{r^2}+1\right)P, \tag{9.79b}$$

$$\sigma_{zz} = 2\nu\frac{a^2}{b^2-a^2}P. \tag{9.79c}$$

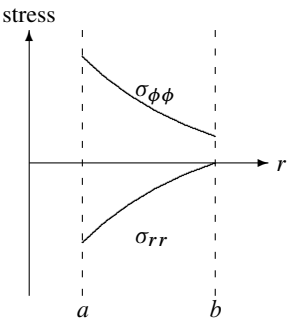

Sketch of stress components.

None of the stresses depend on Young's modulus E, and only the longitudinal stress depends on depends on Poisson's ratio, ν.

The radial pressure, $p_r = -\sigma_{rr}$ can never become larger than P, because we may write

$$\frac{p_r}{P} = \frac{b^2 - r^2}{b^2 - a^2}\,\frac{a^2}{r^2}, \tag{9.80}$$

which is the product of two factors, both smaller than unity for $a < r < b$. The tangential pressure $p_\phi = -\sigma_{\phi\phi}$ and the longitudinal pressure $p_z = -\sigma_{zz}$ are both negative (tensions), and can become large for thin-walled pipes. The average pressure

$$p = \frac{1}{3}\left(p_r + p_\phi + p_z\right) = -\frac{2}{3}(1+\nu)\frac{a^2}{b^2 - a^2}P \tag{9.81}$$

is also negative and like the longitudinal pressure is constant throughout the material. The average pressure does not vanish at $r = b$, and this confirms the suspicion voiced on page 103 that the pressure behaves differently in a solid with shear stresses than the pressure in a fluid at rest, where it has to be continuous across boundaries in the absence of surface tension.

Blowup: A pipe under pressure blows up if the material is extended beyond a certain limit. Compression does not matter, except for very large pressures. The point where the pipe breaks is primarily determined by the point of maximal local tension. As we have seen, this occurs at the inside of the pipe for $r = a$ where

$$\sigma_{\phi\phi} = \frac{b^2 + a^2}{b^2 - a^2}P. \tag{9.82}$$

When this tension exceeds the tensile strength in a brittle material, a crack will develop where the material has a small weakness, and the pipe blows up from the inside!

Example 9.9 [One-inch water pipe]: A standard American one-inch iron water pipe has $2a = 0.957$ inch and $2b = 1.315$ inch. Taking the yield strength of iron to be 200 MPa = 2000 bar, the blowup pressure becomes $P = 62$ MPa = 620 bar. Even with a safety factor 10, normal water pressures can never blow up such a pipe, as long as corrosion has not thinned the wall too much.

Example 9.10 [Frost bursting]: Broken water pipes in winter is a common phenomenon. The reason is that water expands by about 9% when freezing at 0° C. After freezing, as the temperature falls, it contracts slowly. The bulk modulus of solid ice is $K = 8.8$ GPa $= 88,000$ bar. If the water is prevented from expanding along the pipe, for example being blocked by already frozen regions, it will in principle be able to develop a radial pressure of about 9% of the bulk modulus, or $8,000$ bar, which is four times larger than the yield strength of iron. No wonder that pipes burst. The calculation is, however, only an estimate, because other phases of ice exist at high pressures.

Unclamped pipe

In older houses where central heating pipes have been clamped too tight by wall fixtures, major noise problems can arise because no normal fixtures can withstand the large pressures that arise when the water temperature changes and the pipes expand and contract longitudinally. In practice pipes should always be thought of as being unclamped.

The constancy of the longitudinal tension (9.79c) permits us to solve the case of an unclamped pipe by superposing the above solution with the displacement field for uniform stretching (8.23) on page 133. In the cylindrical basis the field of uniform stretching becomes (after interchanging x and z)

$$u_r = -\nu r\frac{Q}{E}, \qquad u_z = z\frac{Q}{E}, \tag{9.83}$$

where Q is the tension applied to the ends.

Choosing Q equal to the longitudinal tension (9.79c) in the clamped pipe,

$$Q = 2\nu \frac{a^2}{b^2 - a^2} P, \tag{9.84}$$

and subtracting the stretching field from the clamped pipe field (9.77) , we find for the unclamped pipe

$$u_r = \frac{a^2}{b^2 - a^2} \left((1 - \nu) r + (1 + \nu) \frac{b^2}{r} \right) \frac{P}{E}, \tag{9.85a}$$

$$u_z = -2\nu \frac{a^2}{b^2 - a^2} z \frac{P}{E}. \tag{9.85b}$$

The strains are likewise obtained from the clamped strains (9.78a) by subtracting the strains for uniform stretching, and we get

$$u_{rr} = \frac{a^2}{b^2 - a^2} \left(1 - \nu - (1 + \nu) \frac{b^2}{r^2} \right) \frac{P}{E}, \tag{9.86a}$$

$$u_{\phi\phi} = \frac{a^2}{b^2 - a^2} \left(1 - \nu + (1 + \nu) \frac{b^2}{r^2} \right) \frac{P}{E}, \tag{9.86b}$$

$$u_{zz} = -2\nu \frac{a^2}{b^2 - a^2} \frac{P}{E}. \tag{9.86c}$$

The superposition principle guarantees that the radial and tangential stresses are the same as before and given by (9.79) , while the longitudinal stress now vanishes, $\sigma_{zz} = 0$.

Thin wall approximation

Most pipes have thin walls relative to their radius. Let us introduce the wall thickness, $d = b - a$, and the radial distance, $s = r - a$, from the inner wall. In the thin-wall approximation, these quantities are small compared to a, and we obtain the following expressions to leading order for the unclamped pipe.

The radial displacement field is constant in the material whereas the longitudinal one is linear in z,

$$u_r \approx a \frac{a}{d} \frac{P}{E}, \qquad u_z \approx -z\nu \frac{a}{d} \frac{P}{E}. \tag{9.87}$$

The corresponding strains become

$$u_{rr} \approx -\nu \frac{a}{d} \frac{P}{E}, \qquad u_{\phi\phi} \approx \frac{a}{d} \frac{P}{E}, \qquad u_{zz} \approx -2\nu \frac{a}{d} \frac{P}{E}. \tag{9.88a}$$

The strains all diverge for $d \to 0$, and the condition for small strains is now $P/E \ll d/a$. The ratio a/d amplifies the strains beyond naive estimates. Finally, we get the non-vanishing stresses

$$\sigma_{rr} \approx -\left(1 - \frac{s}{d} \right) P, \tag{9.89a}$$

$$\sigma_{\phi\phi} \approx \frac{a}{d} P. \tag{9.89b}$$

The radial pressure $p_r = -\sigma_{rr}$ varies between 0 and P as it should when s ranges from 0 to d. It is always positive and of order P, whereas the tangential tension $\sigma_{\phi\phi}$ diverges for $d \to 0$. Blowups always happen because the tangential tension becomes excessive.

Problems

9.1 Show that Navier's equation of equilibrium may be written as

$$\nabla^2 \boldsymbol{u} + \frac{1}{1-2\nu} \nabla \nabla \cdot \boldsymbol{u} = -\frac{1}{\mu} \boldsymbol{f}, \tag{9.90}$$

where ν is Poisson's ratio.

9.2 A body made from isotropic elastic material is subjected to a body force in the z-direction, $f_z = kxy$. Show that the displacement field

$$u_x = Ax^2yz, \qquad u_y = Bxy^2z, \qquad u_z = Cxyz^2, \tag{9.91}$$

satisfies the equations of mechanical equilibrium for suitable values of A, B and C.

9.3 A certain gun has a steel barrel of length of $L = 1$ m, a bore diameter of $2a = 1$ cm. The charge of gunpowder has length $x_0 = 1$ cm and density $\rho_0 = 1$ g cm^{-3}. The bullet in front of the charge has mass $m = 5$ g. The expansion of the ideal gases left by the explosion of the charge at $t = 0$ is assumed to be isentropic with index $\gamma = 7/5$. **(a)** Determine the velocity $\dot{x}$ as a function of x for a bullet starting at rest from $x = x_0$. **(b)** Calculate the pressure just after the explosion and when the bullet leaves the muzzle with a velocity of $U = 800$ m s^{-1}. **(c)** Calculate the initial and final temperatures when the average molar mass of the gases is $M_{\text{mol}} = 30$ g mol^{-1}. **(d)** Calculate the maximal strains in the steel on the inside of the barrel when it has thickness $d = b - a = 5$ mm and compare with the tensile strength of the steel. Will the barrel blow up?

9.4 Show that the most general solution to the uniform shear-free bending of a beam is

$$u_x = a_x - \phi_z y + \phi_y z - \alpha\nu x + \tfrac{1}{2}\beta_x \left(z^2 - \nu(x^2 - y^2)\right) - \beta_y \nu xy, \tag{9.92a}$$

$$u_y = a_y + \phi_z x - \phi_x z - \alpha\nu y + \tfrac{1}{2}\beta_y \left(z^2 - \nu(y^2 - x^2)\right) - \beta_x \nu xy, \tag{9.92b}$$

$$u_z = a_z - \phi_y x + \phi_x y + \alpha z - \beta_x xz - \beta_y yz, \tag{9.92c}$$

and interpret the coefficients.

9.5 Calculate the displacement, strain and stress for an evacuated pipe with fixed ends subject to an external pressure P.

9.6 A massive cylindrical body with radius a and constant density ρ_0 rotates around its axis with constant angular frequency Ω. **(a)** Find the centrifugal force density in cylindrical coordinates rotating with the cylinder. **(b)** Calculate the displacement for the case where the ends of the cylinder are clamped to prevent change in length and the sides of the cylinder are free. **(c)** Show that the tangential strain always corresponds to an expansion, whereas the radial strain corresponds to an expansion close to the center and a compression close to the rim. Find the point, where the radial strain vanishes. **(d)** Where will the breakdown happen?

9.7 Show that a shift in the x-coordinate, $x \to x - \alpha$, in the shear-free bending field (9.19) corresponds to adding in a uniform stretching deformation (plus a simple translation).

9.8 Consider the Navier-Cauchy equation with a point force $\boldsymbol{f} = \boldsymbol{\mathcal{F}}\delta(\boldsymbol{x})$ at the origin. Show that the solution takes the form

$$\boldsymbol{u}(\boldsymbol{x}) = \frac{\boldsymbol{\mathcal{F}}}{4\pi\mu\,|\boldsymbol{x}|} + \frac{\boldsymbol{x} \times (\boldsymbol{x} \times \boldsymbol{\mathcal{F}})}{16\pi\mu(1-\nu)\,|\boldsymbol{x}|^3} \tag{9.93}$$

9.9 Determine the range of values b/a for which the shell actually thickens.

9.10 Calculate how a spherical shell is deformed under its own gravity.